DOI: 10.18462/iir.icr.2023.0647

Evaluation of CO_2-doped blends in single-stage with IHX and parallel compression refrigeration architectures

Manel MARTÍNEZ-ÁNGELES[(a)], Emanuele SICCO[(b)], Gabriele TOFFOLETTI[(b)], Laura NEBOT-ANDRÉS [(a)], Daniel SÁNCHEZ [(a)], Ramón CABELLO [(a)], Giovanni CORTELLA[(b)], Rodrigo LLOPIS [(a)]*

[(a)] Thermal Engineering Group, Mechanical Engineering and Construction Department, Jaume I University Castelló de la Plana,12006, Spain

[(b)] Dipartimento Politecnico di Ingegneria e Architettura, Università degli Studi di Udine, Italy

*Corresponding author: rllopis@uji.es

ABSTRACT

CO_2 refrigeration systems are used worldwide for medium to large applications as they are environmentally friendly and have high security. Lately, the introduction of another refrigerant in small quantities to CO_2 has aroused interest in scientific ambits, since CO_2 mixed with fluids whom critical temperatures are higher permits the cycle move from transcritical conditions to subcritical with the consequent increments of COP in comparison to that of pure CO_2. This work proposes a theoretical study of two of the most CO_2 used cycles, base cycle with internal heat exchanger (IHX) and cycle with parallel compression (PC), working with CO_2-doped mixtures, being the doping agents the fluids R-152a, R-1234yf, R1234ze(E) and R-1233zd(E). The work evaluates cycles energetic performances for an evaporating level of 10ºC and heat rejection temperatures from 20ºC to 40ºC. It anticipated improvements up to 5.8% for the IHX and 10.0% for the PC cycle.

Keywords: Refrigeration, Carbon Dioxide, Refrigerant mixtures, Internal heat exchanger, Parallel compressor

1. INTRODUCTION

Commercial refrigeration has undergone major changes in the last years reaching the current situations where new stand-alone refrigeration systems are based on hydrocarbons (R-600a and R-290), and centralized refrigeration systems on CO_2. However, in the segment that goes from 4kW to 40kW of cooling capacity there are no applicable solutions yet as HCs are not suitable for this purpose because of charge limitations (Calleja-Anta et al., 2021; International Electrotechnical Commission, 2019).

During recent years, there has been a rising interest in extending the use of CO_2 for medium capacity refrigeration systems by using simple configurations with mixtures. Kim et al. (2008) measured improvements of an air-conditioning system using CO_2/propane mixture. This pointed that doping CO_2 with small quantities of other refrigerants can improve energetic performance of refrigeration cycles and several theoretical studies have been conducted on this matter: Zhao et al. (2022) evaluated the use of butane, isobutane and two pure HFOs as CO_2 doping agents for application in single-stage and two-stage cycles with IHX for LT applications. Xie et al. (2022) extended the analysis considering R-152a and R-161 for its application in a single-stage cycle. Finally, Vaccaro et al. (2022) extended the analysis with three hydrocarbons (R-600a, R-600 and R-290) and three hydrofluoroolefins (R-1234ze(E), R-1234ze(Z) and R-1233zd(E)). This is the widest theoretical evaluation to date, as it covers the application of CO_2-doped blends in the single-stage cycle with an IHX, a flash-gas separator, and an ejector.

This work broadens the analysis, focusing the evaluation on R-152a, R-1234yf, R-1234ze(E) and R-1233zd(E) as CO_2 doping agents, simulating the two most simple and used CO_2 architectures: the cycle with double-

stage expansion and internal heat exchanger and the cycle with parallel compression. The work extends the evaluation conditions for an evaporating level of -10ºC and an environment temperature range from 10ºC to 40ºC. Additionally, the work considers the phenomenon of fractionation of the refrigerant in the parallel compression system, which is important parameter to focus on.

2. PROPERTIES OF DOPED CO_2

The benefits of using CO_2 as refrigerant contrast with its low critical temperature, which impede its ability to provide high cooling capacity and good efficiency at high ambient temperatures, as well as its high pressure, which increases the design challenge. By doping CO_2 with small proportions of other fluids, the thermodynamic properties can be adjusted. Refprop is generally used to evaluate the thermophysical properties (Lemmon E. W. et al., 2018). However, it should be noted that mixture properties are estimated through mixing rules based on four adjustable parameters to the Helmholtz energy and one binary-specific multiplier (Bell et al., 2021). They are fitted using published data (experimental or molecular simulation results) by an automatic fitting procedure (Bell and Lemmon, 2016) and when experimental data is not available, the interaction parameters are estimated using the Lemmon and McLinden method (Lemmon and McLinden, 2001) or using interaction parameters for 'similar' blends.

Several CO_2-based mixtures are proposed in this work. Some of the additives are F-gases (R-152a). However, for all considered cases the resultant mixture has a GWP below 150 and they agree with all uses allowed by the F-gas regulation. Other additives (R-1233zd(E), R-1234ze(E) and R-1234yf) are classified as per- and polyfluoroalkyl substances or PFAs. Although for the moment there are no restrictions to their use, it can be that in the near future they will be banned in some applications due to the generation of TFA when they are discomposed in the atmosphere.

Table 1 summarises some thermodynamic properties of different refrigerant blends used in this work, which are calculated for a phase change temperature of -10ºC. Calculated t_C values are higher than CO_2 value, and p_C always rises contrary to the hoped-for behaviour. This could be a deviation of the mixing rules or the correct experimental behaviour. For instance, experimental data of Juntarachat et al. (2014) reports for the mixture CO_2/R-1234yf (89/11% by mass) a p_C of 73.55 bar against 78.41 bar evaluated by Refprop, while for CO_2/R-152a (87/13% by mass) the p_C evaluated by the database (75.53 bar) matches fine the experimental measurement (74.75 ± 0.006 bar) (Madani et al., 2008). This indicates that when estimating the thermophysical properties of the mixtures, some uncertainty is associated, which needs to be considered until experimental validation of the simulations is offered.

Table 1. Thermophysical properties evaluated with Refprop v.10

Fluid	t_C (ºC)	p_C (bar)	λ* (kJ·kg^{-1})	v* (m^3·kg^{-1})	Glide * (K)
CO_2	30.978	73.77	258.61	0.01405	0
R-152a	113.26	45.17	316.98	0.17090	0
CO_2/R-152a [90/10 %]	41.58	78.82	284.61	0.01760	13.3
R-1234yf	94.70	33.82	169.46	0.07962	0
CO_2/R-1234yf [90/10 %]	37.85	77.61	259.45	0.01530	7.3
R-1234ze(E)	109.36	36.35	193.35	0.12301	0
CO_2/R-1234ze(E) [90/10 %]	39.62	78.78	270.38	0.01618	12.4
R-1233zd(E)	166.45	36.24	208.32	0.5423	0
CO_2/R-1233zd(E) [90/10 %]	43.025	83.42	283.08	0.0174	24.2

* Properties evaluated at t=-10ºC and for v as saturated vapour

Fig. 1 depicts the pressure-enthalpy diagram of CO_2 and the mixtures with 10% of additive mass proportion, as well as -10ºC and 30ºC isotherms. It is observed that, for the same phase-change temperatures, the doped mixtures have lower pressures than pure CO_2. With exception of blend CO_2/R-1234yf, all the rest of fluids

have larger latent heats of phase change than CO_2 and the specific volume of saturated vapour increases (Table 1).

On the other hand, an important drawback of the mixtures is the presence of a large glide in the phase-change process; in this case, for a temperature of -10ºC (pressure evaluated for 50% of vapour quality), the glide varies between 7.3 K for the mixture CO_2/R-1234yf [90/10 %] to 24.2 K for CO_2/R-1233zd(E) [90/10 %].

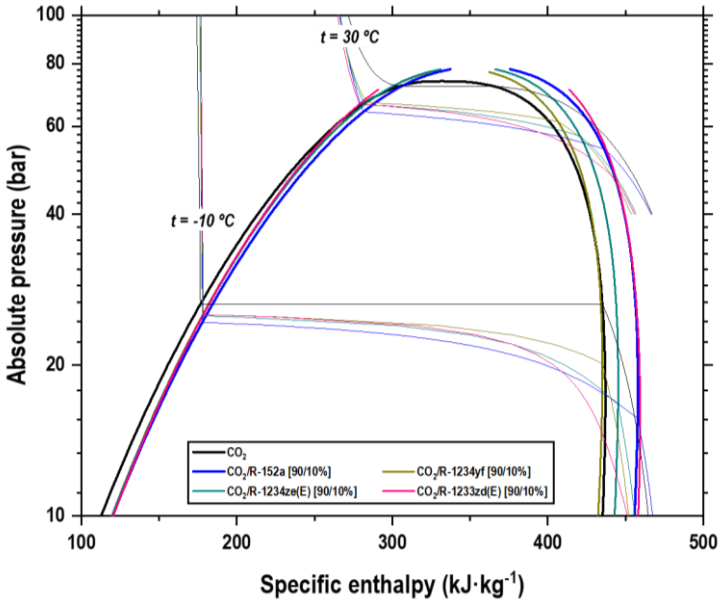

Figure 1. Pressure enthalpy diagram of selected refrigerant blends

3. CYCLE MODELLING

As said previously, the different blends have been simulated with two CO_2 cycles: the base cycle with internal heat exchanger (IHX) which is the standard for cold regions and the cycle with parallel compressor (PC) which is more used in warm regions (Karampour and Sawalha, 2018).

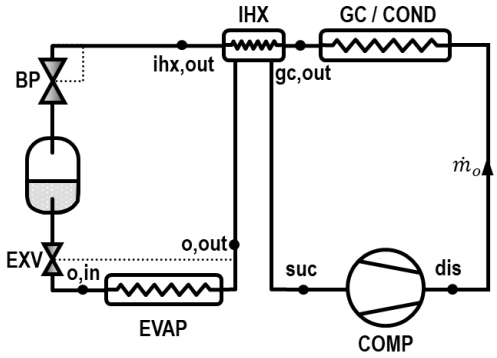

Figure 2. Base cycle with IHX

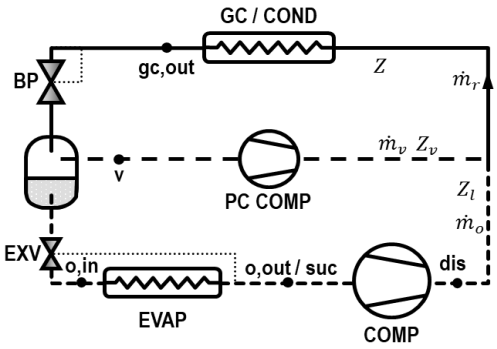

Figure 3. Cycle with parallel compression

3.1. General modelling considerations

Both architectures, using pure CO_2 and blends, were simulated using a first-law approach at the same operating conditions, neglecting heat losses, pressure drops, and avoiding the modelling of the heat exchangers. For a given evaporating temperature (t_o), the low working pressure (p_o) was computed considering the mean enthalpy in the evaporator to consider the glide effects of the blends, Eq. (1).

$$p_o = f\left(t_o, \frac{h_{o,in} + h_v}{2}\right) \qquad \text{Eq. (1)}$$

The heat rejection level was related to the environment temperature (t_{env}), differentiating between subcritical and transcritical operation.

For cycles working in subcritical conditions at low heat rejection temperatures, the temperature at the exit of the condenser ($t_{k,out}$) was calculated considering an approach temperature with the environment (Δt_{sub}) as shown in Eq.(2). The condensing pressure (p_k), fixed by the BP, was considered a degree of freedom and the corresponding condensing temperature (t_k) was evaluated for this pressure and for a quality (x_v) of 50%.

$$t_{k,out} = t_{env} + \Delta t_{sub} \quad \text{Eq. (2)}$$

$$t_k = f(p_k, x_v = 0.5, Z) \quad \text{Eq. (3)}$$

Operation of both cycles in transcritical conditions are carried out at environment temperatures close to or above the critical temperature of each fluid. Therefore, the outlet gas-cooler temperature ($t_{gc,out}$) was determined using a constant temperature difference with the environment (Δt_{trans}) and the heat rejection pressure is also a degree of freedom under these conditions.

$$t_{gc,out} = t_{env} + \Delta t_{trans} \quad \text{Eq. (4)}$$

Evaporator outlet temperature was calculated considering a constant superheating degree (RU), being the reference the saturated vapour temperature at the corresponding pressure ($t_v|_{p_o}$) as shown in the Eq. (5).

$$t_{o,o} = t_v|_{p_o} + RU \quad \text{Eq. (5)}$$

Lamination process is considered isenthalpic, being the enthalpy at vessel liquid exit identical to that of the inlet of the evaporator as pointed in Eq. (6).

$$h_{o,in} = h_l|_{p_i} \quad \text{Eq. (6)}$$

The power consumption of the main compressor ($P_{C,main}$) was calculated considering the refrigerant mass flow ($\dot{m}_o$), the specific isentropic compression work ($w_{s,main}$), and the overall efficiency of the compressor (η_g), which was computed using Eq. (7). The overall effectiveness of the main compressor was obtained with Eq. (8) from manufacturer data (Nebot-Andrés et al., 2019), with its coefficients detailed specified in Eq. (8).

$$P_{C,main} = \dot{m}_o \cdot w_{s,main} \cdot {\eta_g}^{-1} \quad \text{Eq. (7)}$$

$$\eta_g = 0.76339328 - 0.00209763 \cdot p_o + 0.00134440 \cdot p_{gc} - 0.05713840 \cdot p_{gc} \cdot {p_o}^{-1} + 0.54246804 \cdot v_{suc} \quad \text{Eq. (8)}$$

3.2. Specific considerations for the base cycle with IHX

Thermal effectiveness [Eq. (9)] was used to carry out the simulation of IHX. Therefore, through the energy balance in the IHX, Eq. (10); and considering isenthalpic lamination both the volumetric cooling capacity (VCC) and the COP of this architecture are calculated by Eq. (11) and Eq. (12).

$$\varepsilon = \left(t_{suc} - t_{o,out}\right) \cdot \left(t_{gc,out} - t_{o,out}\right)^{-1} \quad \text{Eq. (9)}$$

$$h_{gc,out} - h_{ihx,out} = h_{suc} - h_{o,out} \quad \text{Eq. (10)}$$

$$VCC = \left(h_{o,out} - h_{o,in}\right) \cdot {v_{suc}}^{-1} \quad \text{Eq. (11)}$$

$$COP = \dot{Q}_o \cdot {P_{C,main}}^{-1} = \left(h_{suc} - h_{gc,out}\right) \cdot \eta_g \cdot {w_{s,main}}^{-1} \quad \text{Eq. (12)}$$

The optimization parameter for both transcritical and subcritical conditions with forced condensing pressure is the heat rejection pressure, as the back-pressure valve provides the necessary pressure drop to ensure the subcooling degree of the IHX and to guarantee the minimum compression ratio in the compressor.

3.3. Specific considerations for the parallel compression cycle

The main consideration for performing the simulation of parallel compressor cycle is the steady-state conditions in the vessel. Then, the auxiliary or parallel compressor remove all the vapor exiting the BP valve and all the liquid is sent to the evaporator. For this configuration the vessel pressure is an additional degree of freedom/ parameter of optimization.

The quality at the inlet of the vessel (x_v) was calculated considering the enthalpy at the gas-cooler outlet and the selected/optimized pressure in the vessel according to Eq. (13). Consequently, the vapor mass flow rate can be quantified with Eq. (14) and the liquid flow rate with Eq. (15) since the receiver is in steady-state conditions.

$$x_v = f(p_i, h_{gc,o}, Z) \quad \text{Eq. (13)}$$

$$\dot{m}_v = \dot{m}_r \cdot x_v \quad \text{Eq. (14)}$$

$$\dot{m}_o = \dot{m}_r \cdot (1 - x_v) \quad \text{Eq. (15)}$$

An important and specific consideration for the PC configuration is required when operating with zeotropic blends: the fractionation of the mixture caused by the phase separation in the vessel.

For a given refrigerant composition Z of the refrigerant, when it is fractionated in the vessel, the vapor will have a composition Z_v richer in the most volatile component and the liquid Z_l richer in the least volatile component. Fractionation was calculated using Bell & Deiters' (2018) correlations developed for closed systems, since to the knowledge of the authors there are not specific studies about fractionation dealing with steady flow devices such as the ones considered. The rules for fractionation are available in Refprop (Lemmon E. W. et al., 2018); thus, the mass compositions of saturated vapour and liquid are a function of the vessel pressure, the enthalpy of the mixture at the exit of the back-pressure, and of the initial composition of the refrigerant Z, as detailed by Eq. (16). Accordingly, all the thermodynamic properties from the exit of the liquid of the vessel up to the joint of the two compressors in Fig. 3 were evaluated with the fractionated liquid composition Z_l and those at the auxiliary compressor suction and discharge with the fractionated vapour composition Z_v.

$$[Z_l, Z_v] = f(p_i, h_{gc,out}, Z) \quad \text{Eq. (16)}$$

The volumetric cooling capacity provided by this architecture was evaluated using Eq. (17) considering isenthalpic lamination and its COP with Eq. (18). To evaluate the power consumption of the auxiliary compressor, the same relation for the overall effectiveness presented in Eq. (8) was used.

$$VCC = \left(h_{o,out} - h_{o,in}\right) \cdot {v_{suc}}^{-1} \quad \text{Eq. (17)}$$

$$COP = \dot{Q}_o \cdot (P_{C,main} + P_{C,aux})^{-1} \quad \text{Eq. (18)}$$

Optimization parameters for this architecture are the heat rejection pressure as in the IHX cycle and the vessel or intermediate pressure.

3.4. **Boundary conditions and component limitations**

For the simulations to be a realistic approach the following parameters/conditions are set:

- Approach temperature in gas-cooler/condenser: the approach temperature, in transcritical and forced condensation conditions, was fixed to 2 K due to the high heat transfer rates; in subcritical conditions increased to 4 K for all the refrigerants.
- Superheating degree in evaporator: it was fixed for all the conditions at 5 K.
- Minimum compression ratio: in subcritical conditions at low heat rejection temperatures, a minimum compression ratio of 1.5 was fixed to guarantee the operation of the compressor (Catalán-Gil et al., 2019). For the PC compressor the minimum compression ratio was 1.5 and maximum suction pressure of 55 bar.
- Minimum pressure drop in the expansion valve of the evaporator: 3 bar to guarantee the proper operation of this expansion valve (Catalán-Gil et al., 2019).
- Thermal effectiveness of the IHX was fixed to 50% (Torrella et al., 2011).
- Heat losses to the environment and pressure drops in the components were neglected.

4. RESULTS

This section collects the results from all carried out simulations split in two sub-sections. The first one summarizes the results of the IHX cycle while the second one presents the results obtained from PC cycle for all the simulated fluids at different environment temperatures.

4.1. Cycle with internal heat exchanger

For a given operating condition, the energetic performance of the base cycle when doping CO_2 with another fluid tends to enhance the COP. Fig. 4 depicts the evolution of this parameter (at t_o=-10 ºC, t_{env}=30 ºC) in transcritical conditions. It has been observed that COP increases up to a maximum, beyond which, the addition of more additive results in detriments. Nonetheless, it is clearly observed that CO_2 doping with a small quantity of another fluid (between 10 to 15% for this condition) is a feasible method to enhance CO_2 refrigeration plants performance. Optimum mass proportion calculation was extended to a wide range of operating conditions for the pair CO_2/R-152a, the results of which are presented in Fig. 5. As it can be observed, the optimum composition of additive refrigerant (Z) is practically a function of the heat rejection level, whereas the evaporating temperature has little influence. That is to say, from Fig. 5, it can be affirmed that the use of CO_2-doped mixtures is beneficial at high heat rejection temperatures, especially for environment temperatures higher than 20 ºC, whereas for low heat rejection levels, the use of blends could be even detrimental.

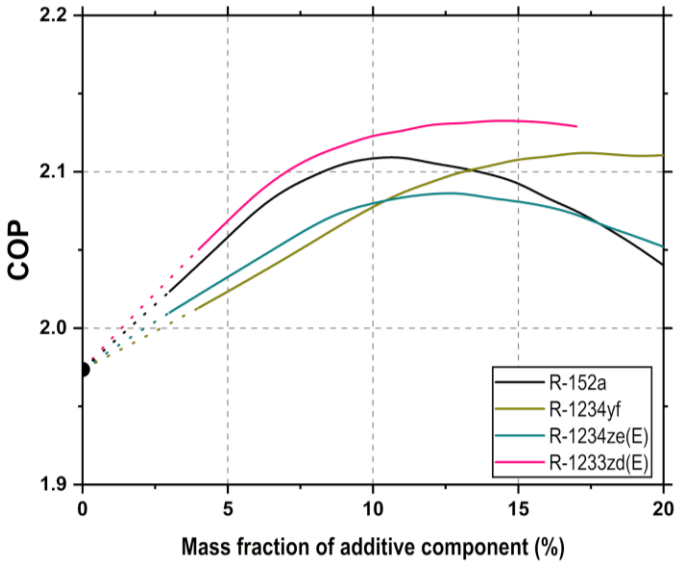

Figure 4. COP of cycle with IHX at t_o=-10 ºC, t_{env}=30 ºC (dotted line in transcritical; continuous line in subcritical with forced condensing pressure)

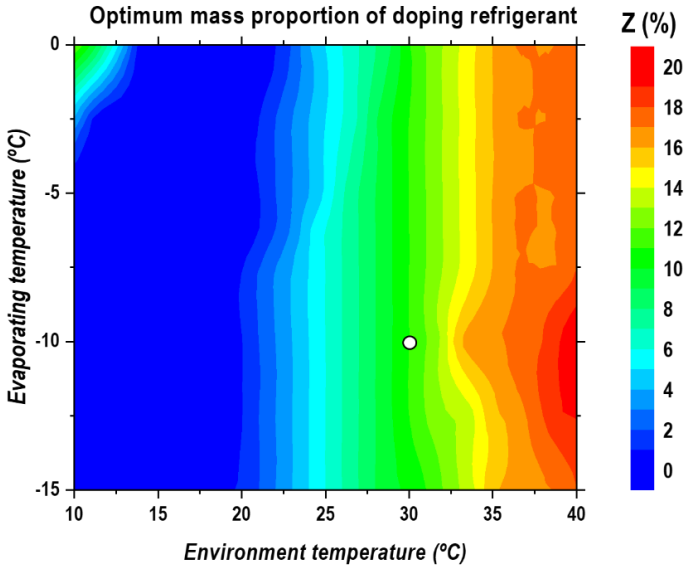

Figure 5. Optimum proportion of R-152a in CO_2 with the IHX cycle at different operating levels

Fig. 6 depicts the operating cycle of the base system in a p-h diagram at the best performing conditions. As can be noted, the CO_2 cycle operates in transcritical conditions, where the back-pressure regulates the heat rejection pressure. When adding 10% of R-152a, p_c, t_c and the cycle move to subcritical operation where the back-pressure forces the condensing level to maintain the subcooling degree of the internal heat exchanger, which is the condition that maximizes the COP. The COP achieved with the blend is 6.9% higher than with CO_2. However, the use of the blend causes a reduction in the VCC of 25.5% because of the lower volumetric capacity R-152a. It is also important to point the reduction of the operating pressures with the blend since, the optimum high pressure is reduced by 10.2 bar and the evaporating level by 5.2 bar. In evaporation, the glide effect can be observed (Fig. 6), which is a disadvantage for the heat transfer process in the evaporator as, for an evaporating temperature of -10ºC the evaporator operates with an effective temperature glide of 12.2 K which will require higher heat transfer surfaces in comparison to the operation with CO_2. Finally, another important modification perceived is a high increase of the compressor discharge temperature.

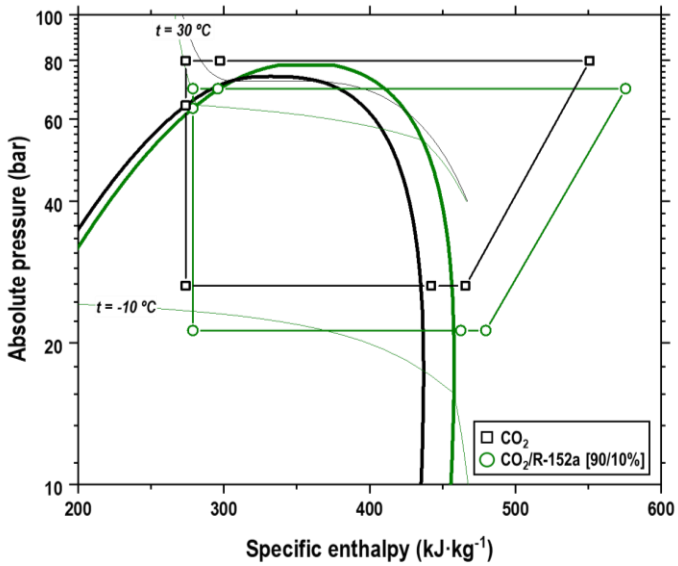

Figure 6. IHX P-h diagram at opt. conditions with CO_2 and CO_2/R-152a [90/10%] (t_o = -10ºC, t_{env} = 30ºC)

Finally, Fig. 7 summarizes the COP deviation of the considered blends (with 5 and 10% proportion) in relation to the operation of the cycle with IHX and CO_2. As mentioned, doping is not advisable for low heat rejection temperatures, as use of all blends present COP reductions. At low temperatures the CO_2 cycle works in subcritical with high efficiency, thus, these blends cause efficiency reductions. Then, at medium heat rejection levels, the COP modification is neutral, coinciding with the transition regime of CO_2 operation. But

at high heat rejection levels (25 to 35ºC), the COP of the system is enhanced using the mixtures, as the doped fluids still operate in subcritical conditions. For the considered fluids, the predicted COP gains at t_o =-10ºC reach between 3.16% at 27ºC (CO_2/R-1234yf [95/5%]) to 7.70% at 31ºC (CO_2/R1233ze(E) [90/10%]).

Authors want to mention that the application of CO_2-doped mixtures could be an opportunity to improve the performance of cycles based on CO_2, particularly at high heat rejection temperatures. Although COP improvements have been predicted, these results need to be validated experimentally, as they rely on the accuracy the mixing rules for estimating the thermophysical properties.

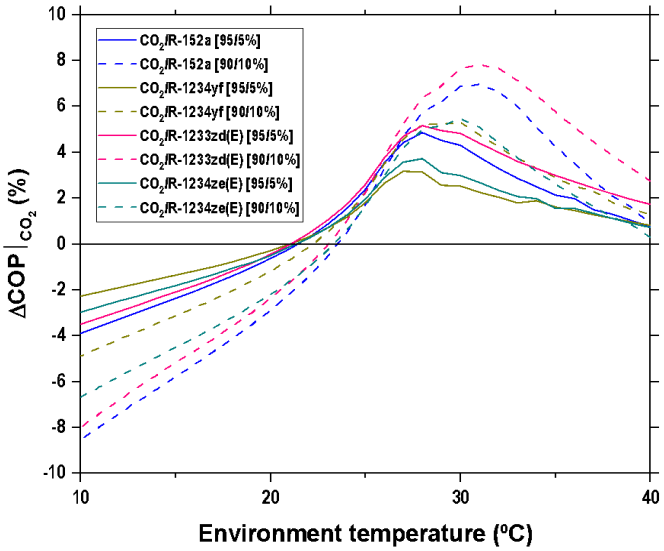

Figure 7. COP percentage difference from pure CO_2 with base cycle with IHX at t_o = -10 ºC

4.2. Cycle with parallel compression

As mentioned, the state-of-the-art cycle for medium and high heat rejection level corresponds to the cycle with parallel compression, wherein the auxiliary compressor's function is to remove the vapour generated in the vessel, increasing the specific cooling capacity and thus enhancing cycle's energy efficiency (Karampour and Sawalha (2018) and Nebot-Andrés et al. (2021)). When blends are used as refrigerants, this architecture has special features, as the vessel will experience fractionation. Phase-separation in the vessel will provide two currents with different compositions: the saturated vapor will contain a higher proportion of the most volatile component, and the saturated liquid will contain a higher proportion of the least volatile component.

To illustrate the use of blends in the parallel compression architecture, we focus on the operation of the cycle at t_o=-10 ºC and t_{env}=30 ºC. Fig. 9 depicts the p-h diagram at optimum conditions for the mixture CO_2/R-1233zd(E) [90/10%]. It is observed that, as with the IHX cycle, CO_2 doping moves the cycle from transcritical to subcritical operation (Fig. 9), introducing the positive effects mentioned in Subsection 4.1. Fractionation produces two different currents: saturated vapour extracted from the vessel has a composition of CO_2/R-1233zd(E) [97.71/2.29%] and saturated liquid of CO_2/R-1233zd(E) [86.39/13.61%]. These compositions reveal that, thanks to the fractionation, two different refrigerants are generated, whose properties can enhance or worsen the performance of the cycle. It is desirable for the vapour current to contain more of fluid with less slope in the isentropic lines while for the liquid flow is preferable to present higher volumetric cooling capacity, to increase the cooling effect in the evaporator. These effects, which are clear when considered separately, cannot be isolated in the considered cycle; thus, a complete evaluation at optimum conditions is needed. For the considered case (Fig. 9), the use of the blend theoretically enhances the COP of the cycle by 1.8% at these conditions (7.7% in IHX cycle), so it appears that the improvements of doping are lower for this architecture.

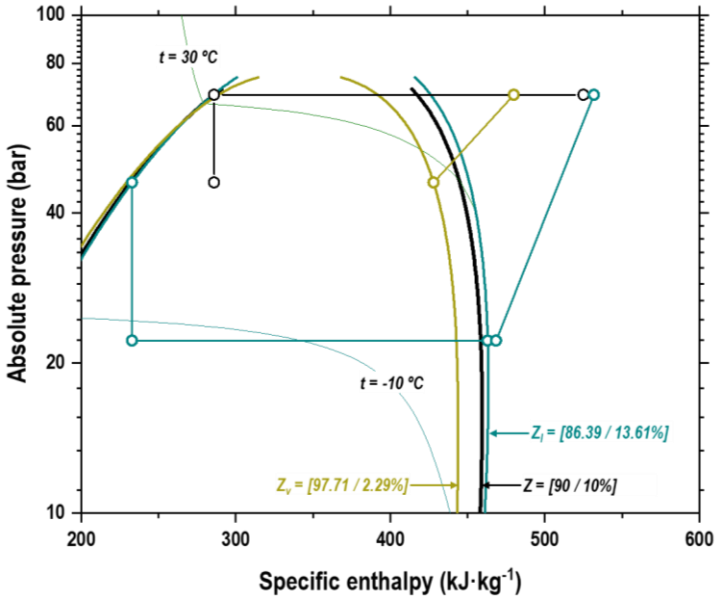

Figure 8. PC cycle P-h diagram at opt. cond. with CO_2/R-1233zd(E) [90/10%] (t_o = -10ºC, t_{env} = 30ºC)

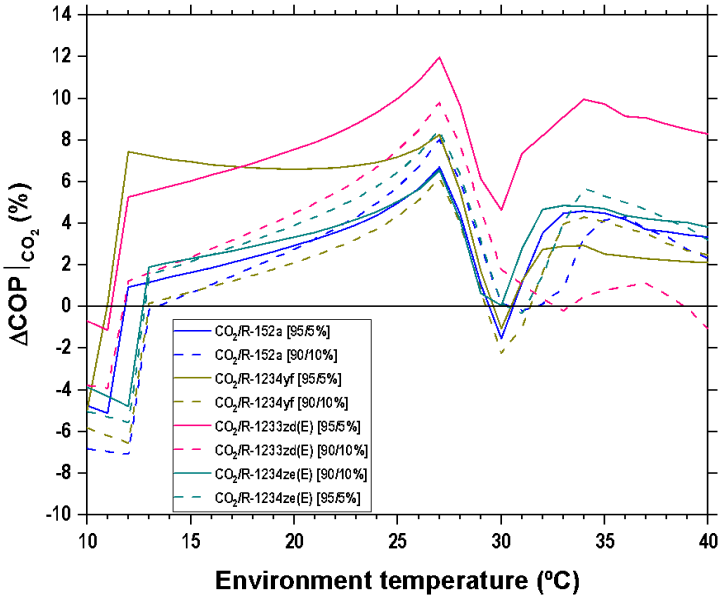

Figure 9. COP percentage difference from pure CO_2 with PC cycle at t_o = -10 ºC

Fig. 9 summarizes the COP deviation of the considered blends (with 5 and 10% proportion) in relation to the operation with CO_2. The trends are quite different from the operation with the IHX cycle. First, at low heat rejection levels (up to t_{env} = 13 ºC) the auxiliary compressor does not operate because the compression ratio is below 1.5. In this region, as well as in the IHX cycle, doping is not convenient. From this temperature up to 27ºC approximately, the auxiliary compressor operates and there is fractionation in the cycle (see Fig. 10.). In this region there is a clear trend of COP improvement when using CO_2-doped blends. When the auxiliary compressor starts, the vapor line (the one that compresses the auxiliary compressor) contains a higher proportion of the most volatile component, in this case CO_2, and the liquid line higher proportion of the least volatile component. Calculations predict COP improvements up to 11.98% (CO_2/R1233zd(E) [95/5%]) at t_{env} = 27 ºC. In this region all the blends offer COP improvements. From 27 to 32 ºC approximately, there is a big reduction in the enhancement. Finally, from temperatures above 32ºC the COP enhancement stabilises, from 2% approximately for CO_2/R1234yf [95/5%] to 8% approximately with CO_2/R1233ze(E) [95/5%].

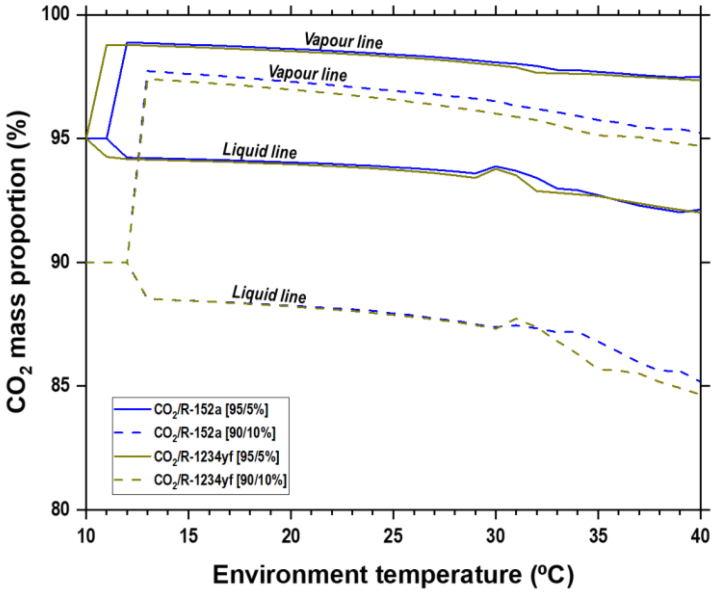

Figure 10. CO_2 mass proportion in currents after fractionation for mixtures CO_2/R-152a and CO_2/R-1234yf with PC cycle at t_o = -10 ºC

Authors want to mention that the theoretical approach is subjected to an unknown degree of uncertainty and an experimental validation is needed.

5. CONCLUSIONS

This work addresses, using a theoretical approach, the use of CO_2-doped blends as a possible improvement of two classical CO_2 cycles, the internal heat exchanger and parallel compression. Here, R-152a, R-1234yf, R-1234ze(E) and R-1233zd(E) have been considered as doping agents to modify the performance of the selected architectures. Results have been based on the use of a comprehensive and simplified model using Refprop v.10 and its mixing rules as reference.

It has been predicted that 5-10% CO_2 doping tends to enhance the COP of the architectures, but this is accompanied by a reduction of the volumetric cooling capacity. The optimum mass proportion of additive is independent on the evaporating level, being only dependent and positive for environment temperatures above 20ºC. CO_2 doping with pure fluids which have higher critical temperature allows the optimum condition of the cycle to go to subcritical operation, causing a reduction of the operating pressures in all the cycles.

Considering the IHX architecture, COP improvements are predicted in environment temperatures higher than 25 ºC, reaching maximum improvement around 30 ºC and being attenuated at 40 ºC. For the analysed blends, the COP gains at t_o=-10 ºC reach between 3.16% at 27 ºC (CO_2/R-1234yf [95/5%]) to 7.70% at 31 ºC (CO_2/R1233ze(E) [90/10%]).

In relation to the PC layout, the use of refrigerant blends deals with the fractionation of the refrigerant in the phase-separation vessel, where two currents with different compositions are generated. The saturated vapour contains a higher proportion of the most volatile component (CO_2 in this work), and the saturated liquid is enriched with the least volatile component (doping agents in this work). This fractionation introduces modifications to the cycle, which can be considered as another mechanism to enhance the performance. For the PC cycle, CO_2-doped has wider range of benefit, approximately from t_{env}=13 ºC to 27 ºC and from 32 to 40 ºC. Also, the COP enhancement is higher with this architecture. Enhancements up to 11.98% were predicted with the mixture (CO_2/R1233zd(E) [95/5%]) at t_{env}=27 ºC.

Finally, the authors want to mention that CO_2 doping, which has only been considered theoretically up to this point, could represent a new way of improving the energy performance of low-GWP refrigeration systems. The authors want to emphasize that an experimental validation is required to confirm this hypothesis.

ACKNOWLEDGEMENTS

This article is part of the project TED2021-130162B-I00, funded by MCIN/AEI/10.13039/501100011033 and by the European Union - NextGenerationEU "NextGenerationEU"/PRTR.

Authors want to acknowledge the economic support to this study by the European Union – "NextGenerationEU" (L. Nebot, Margarita Salas postdoctoral contract MGS/2022/15; M. E. Martínez, grant INVEST/2022/294; by the Ministerio de Ciencia e Innovación of Spain (project PID2021-126926OB-C21) and by Jaume I University (project UJI-B2021-10). The research leading to these results has also received funding from the MIUR of Italy within the framework of the PRIN2017 project «The energy flexibility of enhanced heat pumps for the next generation of sustainable buildings (FLEXHEAT)», grant 2017KAAECT.

NOMENCLATURE

BP	back-pressure valve
COP	coefficient of performance
COMP	compressor
COND	condenser
CR	compression ratio
EVAP	evaporator
EXV	expansion valve
GC	gas-cooler
H	specific enthalpy (kJ·kg^{-1})
IHX	internal heat exchanger
LT	low temperature level
$\dot{m}$	mass flow rate (kg·s^{-1})
MT	medium temperature level
p	pressure (bar)
PC	parallel compressor
P_C	power consumption (W)
p_C	critical pressure (bar)
p_i	vessel pressure (bar)
$\dot{Q}_o$	cooling capacity (W)
RU	superheat in the evaporator (k)
t	temperature (ºC)
t_C	critical temperature (ºC)
VCC	volumetric cooling capacity (kJ·kg^{-1})
w_S	specific isentropic compression work (kJ·kg^{-1})
x	quality
Z	mass fraction of components
Z_v	mass fraction of components of saturated vapour
Z_l	mass fraction of components of saturated liquid
ε	thermal effectiveness
η_g	overall efficiency of the compressor
v	specific suction volume (m^3·kg^{-1})

Subscripts

aux	refers to the auxiliary compressor
dis	refers to compressor discharge
env	refers to environment
in	inlet
k	condenser
l	saturated liquid
main	refers to main compressor
o	refers to evaporator
out	outlet
sub	subcooling
suc	compressor suction
trans	refers to transcritical operation
v	saturated vapour

REFERENCES

Bell, I.H., Lemmon, E.W., 2016. Automatic Fitting of Binary Interaction Parameters for Multi-fluid Helmholtz-Energy-Explicit Mixture Models. Journal of Chemical & Engineering Data 61, 3752-3760.

Bell, I.H., Riccardi, D., Bazyleva, A., McLinden, M.O., 2021. Survey of Data and Models for Refrigerant Mixtures Containing Halogenated Olefins. Journal of Chemical & Engineering Data 66, 2335-2354.

Calleja-Anta, D., Nebot-Andrés, L., Cabello, R., Sánchez, D., Llopis, R., 2021. A3 and A2 refrigerants: Border determination and hunt for A2 low-GWP blends. International Journal of Refrigeration Under revision.

Catalán-Gil, J., Llopis, R., Sánchez, D., Nebot-Andrés, L., Cabello, R., 2019. Energy analysis of dedicated and integrated mechanical subcooled CO2 boosters for supermarket applications. International Journal of Refrigeration 101, 11-23.

International Electrotechnical Commission, 2019. Voting Result 61C/792/FDIS, SC 61C Safety of refrigeration appliances for household and commercial use.

Juntarachat, N., Valtz, A., Coquelet, C., Privat, R., Jaubert, J.-N., 2014. Experimental measurements and correlation of vapor–liquid equilibrium and critical data for the CO2 + R1234yf and CO2 + R1234ze(E) binary mixtures. International Journal of Refrigeration 47, 141-152.

Karampour, M., Sawalha, S., 2018. State-of-the-art integrated CO 2 refrigeration system for supermarkets: A comparative analysis. International Journal of Refrigeration 86, 239-257.

Kim, J.H., Cho, J.M., Kim, M.S., 2008. Cooling performance of several CO2/propane mixtures and glide matching with secondary heat transfer fluid. International Journal of Refrigeration 31, 800-806.

Kim, M.H., Pettersen, J., Bullard, C.W., 2004. Fundamental process and system design issues in CO2 vapor compression systems. Progress in Energy and Combustion Science 30, 119-174.

Lemmon, E., McLinden, M., 2001. Method for Estimating Mixture Equation of State Parameters, Thermophysical Properties and Transfer Processes of New Refrigerants, Paderborn, -1 (Accessed July 22, 2022).

Lemmon E. W., I.H., B., L., H.M., O., M.M., 2018. NIST Standard Reference Database 23: Reference Fluid Thermodynamic and Transport Properties-REFPROP, Version 10.0, National Institute of Standards and Technology.

Llopis, R., Toffoletti, G., Nebot-Andrés, L., Cortella, G., 2021. Experimental evaluation of zeotropic refrigerants in a dedicated mechanical subcooling system in a CO2 cycle. International Journal of Refrigeration.

Madani, H., Valtz, A., Coquelet, C., Meniai, A.H., Richon, D., 2008. (Vapor+liquid) equilibrium data for (carbon dioxide+1,1-difluoroethane) system at temperatures from (258 to 343)K and pressures up to about 8MPa. The Journal of Chemical Thermodynamics 40, 1490-1494.

Nebot-Andrés, L., Calleja-Anta, D., Sánchez, D., Cabello, R., Llopis, R., 2019. Thermodynamic analysis of a CO2 refrigeration cycle with integrated mechanical subcooling. Energies 13.

Nebot-Andrés, L., Sánchez, D., Calleja-Anta, D., Cabello, R., Llopis, R., 2021. Experimental determination of the optimum intermediate and gas-cooler pressures of a commercial transcritical CO2 refrigeration plant with parallel compression. Applied Thermal Engineering, 116671.

Torrella, E., Sánchez, D., Llopis, R., Cabello, R., 2011. Energetic evaluation of an internal heat exchanger in a CO2 transcritical refrigeration plant using experimental data. International Journal of Refrigeration 34, 40-49.

Vaccaro, G., Milazzo, A., Talluri, L., 2022. Thermodynamic assessment of trans-critical refrigeration systems utilizing CO2-based mixtures. International Journal of Refrigeration.

van Konynenburg P. H., Scott R. L., 1980. Critical lines and phase equilibria in binary van der Waals mixtures. Philosophical Transactions of the Royal Society of London. Series A, Mathematical and Physical Sciences 298 (1442).

Xie, J., Wang, J., Lyu, Y., Wang, D., Peng, X., Liu, H., Xiang, S., 2022. Numerical investigation on thermodynamic performance of CO2-based mixed refrigerants applied in transcritical system. Journal of Thermal Analysis and Calorimetry 147, 6883-6892.

Zhao, Z., Luo, J., Song, Q., Yang, K., Wang, Q., Chen, G., 2022. Theoretical investigation and comparative analysis of the Linde-Hampson refrigeration system using eco-friendly zeotropic refrigerants based on R744/R1234ze(Z) for freezing process applications. International Journal of Refrigeration.